European Journal of
Nuclear
Medicine

Original article

A method to quantitate cerebral blood flow using a rotating gamma camera and iodine-123 iodoamphetamine with one blood sampling

Hidehiro Iida, Hiroshi Itoh, Peter M. Bloomfield, Masahiro Munaka, Shuichi Higano, Matsutaro Murakami, Atsushi Inugami, Stefan Eberl, Yasuo Aizawa, Iwao Kanno, Kazuo Uemura

Research Institute for Brain and Blood Vessels, 6–10 Senshu-kubota-machi, Akita City, Akita, Japan 010

Received 15 August 1993 and in revised form 5 April 1994

Abstract. A method has been developed to quantitate regional cerebral blood blow (rCBF) using iodine-123-labelled *N*-isopropyl-*p*-iodoamphetamine (IMP). This technique requires only two single-photon emission tomography (SPET) scans and one blood sample. Based on a two-compartment model, radioactivity concentrations in the brain for each scan time (early: t_e; delayed: t_d) are described as: $C_t(t_e) = f \cdot C_a(t_e) \otimes e^{-\frac{f}{V_d} \cdot t_e}$ and $C_t(t_d) = f \cdot C_a(t_d) \otimes e^{-\frac{f}{V_d} \cdot t_d}$, respectively, where $\otimes$ denotes the convolution integral; $C_a(t)$, the arterial input function; f, rCBF; and V_d, the regional distribution volume of IMP. Calculation of the ratio of the above two equations and a "table look-up" procedure yield a unique pair of rCBF and V_d for each region of interest (ROI). A standard input function has been generated by combining the input functions from 12 independent studies prior to this work to avoid frequent arterial blood sampling, and one blood sample is taken at 10 min following IMP administration for calibration of the standard arterial input function. This calibration time was determined such that the integration of the first 40 min of the calibrated, combined input function agreed best with those from 12 individual input functions (the difference was 5.3% on average). This method was applied to eight subjects (two normals and six patients with cerebral infarction), and yielded rCBF values which agreed well with those obtained by a positron emission tomography $H_2{}^{15}O$ autoradiography method. This method was also found to provide rCBF values that were consistent with those obtained by the non-linear least squares fitting technique and those obtained by conventional microsphere model analysis. The optimum SPET scan times were found to be 40 and 180 min for the early and delayed scans, respectively. These scan times allow the use of a conventional rotating gamma camera for clinical purposes. V_d values ranged between 10 and 40 ml/g depending on the pathological condition, thereby suggesting the importance of measuring V_d for each ROI. In conclusion, optimization of the blood sampling time and the scanning time enabled quantitative measurement of rCBF with two SPET scans and one blood sample.

Key words: Iodine-123 labelled *N*-isopropyl-*p*-iodoamphetamine – Regional cerebral blood flow – Single-photon emission tomography

Eur J Nucl Med (1994) 21:1072–1084

Correspondence to: H. Iida, Department of Radiology and Nuclear Medicine, Research Institute for Brain and Blood Vessels, 6–10 Senshu-kubota-machi, Akita City, Akita, Japan 010

Introduction

Iodine-123-labelled *N*-isopropyl-*p*-iodoamphetamine (IMP) is used for mapping brain perfusion with single-photon emission tomography (SPET) [1–3]. Because of its relatively high first-pass extraction fraction and high affinity in the brain, the early picture following the intravenous administration of IMP reflects the distribution of regional cerebral blood flow (rCBF), and with arterial blood sampling absolute quantification of the rCBF value is possible. However, the early picture following IMP administration requires rapid completion of a SPET scan, although the accuracy of this data acquisition is sometimes limited, particularly when using a conventional rotating gamma camera. As has been demonstrated by previous investigators [4–10], IMP has significant clearance from the brain, and the regional IMP concentration in the brain changes when initiation of the SPET scan is delayed [4–10]. The clearance of IMP causes a systematic underestimation of the global CBF values and reduction in contrast between high rCBF and low rCBF regions [8].

In order to correct for the clearance of IMP from the brain, a two-compartment model has been recommended

by various authors [6, 9, 11] for describing the IMP kinetics. In these studies, two functional parameters of rCBF and the regional distribution volume of IMP (V_d) were calculated for each regional segment using non-linear least squares fitting. This technique, however, required too laborious procedures, including sequential data acquisition by a dynamic SPET scan following the IMP infusion, frequent arterial blood sampling and separation of the lipophilic fractions for each blood sample, and thus had limited applicability for clinical use.

The purpose of this study was to develop a new method which minimizes the procedures required for calculating both rCBF and regional V_d from a two-compartment model analysis. The mathematical calculation was designed so that only two SPET scans provide two parameters (rCBF and V_d). Frequent arterial blood sampling and separation of the lipophilic fractions were avoided by employing a standard input function. A single blood sample was referenced to standardized input function, derived from an independent study population, in order to determine the value of the arterial input function for each subject at each imaging time. To minimize errors caused by the inter-individual differences of the input function, timing of the SPET scans and timing of the blood sampling were investigated. Finally, the accuracy of the present method was compared with an independent technique using positron emission tomography (PET).

Materials and methods

Theory

Model. The two-compartment model (see Fig. 1a) has been employed in this study according to previous reports [6, 8–11]. Accuracy and limitations of this model will be discussed later.

The rate of change of the radioactivity concentration, $C_t(t)$, in a small element of the brain at a given time t, is therefore expressed as:

$$\frac{dC_t(t)}{dt} = K_1 \cdot C_a(t) - k_2 \cdot C_t(t), \tag{1}$$

where K_1 (milliliters of blood/min per milliliter of ROI) denotes the wash-in rate constant from the blood to the brain, k_2 (1/min) the wash-out (clearance) rate constant from the brain to the blood, and $C_a(t)$ the arterial input function. Assuming that IMP is freely diffusible across the blood-brain barrier (i.e. the first-pass extraction fraction of IMP is unity, E=1), K_1 and k_2 are related to rCBF (ml/min/g) and the regional V_d of IMP (ml/ml) as follows:

$$K_1 = \rho \cdot f \tag{2a}$$

$$k_2 = \frac{K_1}{V_d}, \tag{2b}$$

where ρ denotes the density of the brain tissue (assumed to be 1.04 g/ml in this study), f the rCBF, and V_d the regional distribution volume of IMP. Limitations of the assumption (E=1) will be discussed later. Solving Eq. 1 and inserting Eqs. 2a and 2b into the solution provide the regional tissue radioactivity concentration at time t as:

2-Compartment Model

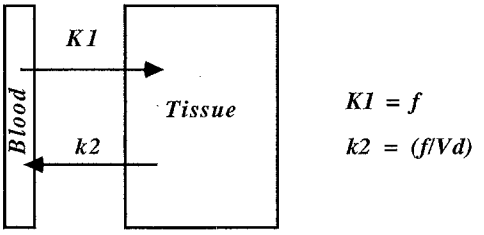

a

3-Compartment Model

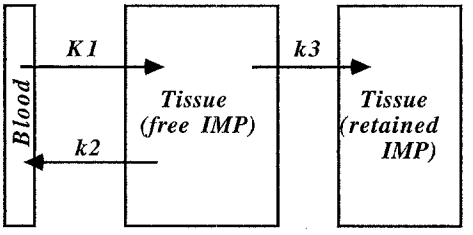

b

Fig. 1. a Two-compartment model employed in the present study. K_1 and k_2 denote the rate constants of the wash-in and the wash-out of IMP between the capillary and the interstitial space, respectively. The rCBF corresponds to K_1, and the regional V_d corresponds to the K_1 to k_2 ratio. **b** Three-compartment model used to validate the two-compartment model for the description of IMP kinetics in the brain. k_3 denotes the retaining rate constant of IMP in the brain tissue. The non-linear least squares fitting was performed to determine each of the K_1, k_2 and k_3 values, and the significance of including the k_3 parameter was evaluated (see text)

$$C_t(t) = \rho \cdot f \cdot C_a(t) \otimes e^{-\frac{f}{V_d} \cdot t}, \tag{3}$$

where $\otimes$ denotes the convolution integral. The radioactivity concentration measured at two different times (the early scan time, t_e, and the delayed scan time, t_d) are given by:

$$C_t(t_e) = \rho \cdot f \cdot C_a(t_e) \otimes e^{-\frac{f}{V_d} \cdot t_e} \tag{4a}$$

$$C_t(t_d) = \rho \cdot f \cdot C_a(t_d) \otimes e^{-\frac{f}{V_d} \cdot t_d} \tag{4b}$$

respectively. Dividing Eq. 4a by Eq. 4b cancels the flow and density terms, and yield the ratio of counts in the early image to that in the delayed image (early-to-delayed ratio) as:

$$\frac{C_t(t_e)}{C_t(t_d)} = \frac{C_a(t_e) \otimes e^{-\frac{f}{V_d} \cdot t_e}}{C_a(t_d) \otimes e^{-\frac{f}{V_d} \cdot t_d}}. \tag{5}$$

Calculation of rCBF. The computation procedure generates a table of the ratio of convolution integral on the right side of Eq. 5 as a function of f/V_d. For a given input function, $C_a(t)$, and given scan time combination (t_e and t_d), this calculation is done only once. Since $C_t(t_e)/C_t(t_d)$ is measured by two SPET scans, a value for f/V_d can be obtained through the "table look-up procedure" using the above calculated table. Therefore, the rCBF value can be calculated as follows:

$$f = \frac{C_t(t_e)}{\Gamma}, \tag{6}$$

ard where Γ is defined as:

$$\Gamma = \rho \cdot C_a(t_e) \otimes e^{-\frac{f}{V_d} \cdot t_e} \tag{7}$$

Another table of Γ can be generated as a function of f/V_d. Using this table together with the above calculated table between $C_t(t_e)/C_t(t_d)$ and f/V_d, a table of Γ can also be generated as a function of $C_t(t_e)/C_t(t_d)$. Thus, the table look-up procedure provides a unique Γ value from the early-to-delayed ratio. The value of rCBF can therefore be calculated as a ratio of the early counts to the Γ value (i.e. Eq. 4a/Eq. 7). The regional distribution volume of IMP can then be calculated as a ratio of f and f/V_d.

In the present method, a standard input function, which has been generated by combining the input functions from 12 independent studies prior to this work (see Appendix 1), was used to avoid frequent arterial blood sampling. A single arterial blood sample was used to calibrate to the standardized input function:

$$C_a(t) = C_f \cdot A(t), \tag{8}$$

where $A(t)$ is the standard input function, and C_f the calibration factor to scale the standard input function in each study. The blood sampling time for the calibration time is determined so as to minimize the inter-individual difference in integration of the input function (see Appendix 2).

Polynomial approximation of the table look-up procedure. In the situation that the shape of the arterial input function is provided, the table look-up procedure described above can be simplified by replacing it by polynomial functions as follows. For a given scan time combination, the table of $C_t(t_e)/C_t(t_d)$ as a function of f/V_d becomes unique, and the table Γ as a function of f/V_d becomes dependent only on the calibration factor (C_f). Using the standard input function described in Appendix 1, the table look-up procedures are replaced by two polynomial functions shown in Appendix 3. When the early scan and the delayed scans were performed at 40 min and 180 min after the IMP infusion, respectively, f/V_d and Γ could be obtained from the early-to-delayed count ratio as:

$$\begin{aligned} f/V_d = & -0.047253 + 0.15931\,X \\ & -0.195045\,X^2 + 0.12179\,X^3 \\ & -0.036247\,X^4 + 0.0041532\,X^5 \end{aligned} \tag{9}$$

$$\begin{aligned} \Gamma = & 43301.1 - 45911.75\,X \\ & + 44139.0\,X^2 - 24485.46\,X^3 \\ & + 6795.5859\,X^4 - 745.6684\,X^5, \end{aligned} \tag{10}$$

where X denotes the ratio of the radioactivity concentration at 40 min to that at 180 min. The rCBF, f, is thereby calculated as:

$$f = \frac{\text{SPET counts at } t_e}{C_f \cdot \Gamma}. \tag{11}$$

Then, calculating a ratio of f to f/V_d provides the regional V_d value.

Three-compartment model. In order to evaluate effects of the retention of IMP in the brain, a model which includes a retention rate constant (k_3) in addition to K_1 and k_2 is formulated based on the three-compartment model (see Fig. 1b). The radioactivity concentration in the brain following the IMP administration is expressed as:

$$C_t(t) = \frac{K_1}{k_2 + k_3} \left\{ k_3 + k_2 \cdot e^{-(k_2 + k_3) \cdot t} \right\} \otimes C_a(t). \tag{12}$$

Method

Simulation. Tissue time-activity curves following the administration of IMP were simulated for various rCBF values using Eq. 3. The standard input function described in Appendix 1 has been used. According to our observation in normal cerebral tissues (see below), the value of V_d was fixed at 30.0 ml/ml.

Tables of k_2 (f/V_d) values and the early-to-delayed count ratios (Eq. 5) were calculated for various scan combination times, namely for mid-scan times of 10 min and 60 min, 20 min and 80 min, 10 min and 180 min, and 40 min and 180 min. The standard input function obtained in Appendix 1 has also been used in this simulation.

Subjects. IMP SPET studies were performed on eight subjects including two normal volunteers and six patients with cerebral infarction (Table 1). None of these subjects belonged to the study group for generating the standard input function described in Appendix 1. All subjects gave written informed consent to a protocol approved by the committee for clinical research of this institute.

Table 1. Subject data

Subject number	Diagnosis	Age (yr)	Sex	SPET scan[a]	PaCO2 (mmHg)		Smoking	Lung function	Heart function/ failure
					SPET[b]	PET			
1	Chronic CI	63	M	A	40.3	40.7	Non	Normal	Normal
2	Acute CI	80	M	A	38.4	39.4	Non	Normal	Normal
3	Acute CI	74	F	A	39.7	37.1	Non	Normal	NYHA-3
4	Chronic CI	71	M	A	40.5	40.1	Non	Normal	Normal
5	Normal	26	M	A	42.2	42.9	Non	Normal	Normal
6	Chronic CI	72	M	B	40.3	40.7	20/day	Normal	Normal
7	Normal	31	M	B	40.3	40.7	Non	Normal	Normal
8	Chronic CI	45	F	B	40.3	40.7	Non	Normal	Normal
Mean		58			40.3	40.2			
± SD		± 22			± 1.1	± 1.7			

CI, Cerebral infarction; M, male; F, female

[a] A, Dynamic SPET scan (group A); B, rotating gamma camera (group B)

[b] Group A, average of four measurements; group B, measurement at 10 min after IMP infusion

The subjects were divided into two groups: group 1 (five subjects) had a dynamic SPET scan on a ring-type SPET system with frequent arterial sampling (see the next subsection), while group 2 (three subjects) underwent only two SPET scans using a rotating gamma camera with one arterial blood sampling.

The first group consisted of one male normal volunteer (age 26) and four patients with cerebral infarction (age: 63-71; three males and one female). Two patients suffered from chronic cerebral infarction and the other two from acute cerebral infarction (days 8 and 6). One acute patient showed chronic heart failure (NYHA grade 3) at the time of the SPET scan. None of them were smokers or showed abnormalities in their lungs.

The second group included one male normal volunteer (age 31) and two patients with chronic cerebral infarction (one male and one female aged 72 and 45, respectively). In this group one male patient was a smoker, but no lung abnormalities were evident in any of the subjects in this group.

Group 1 (dynamic SPET scan). Following a 1-min infusion of 222 MBq IMP, a dynamic SPET scan was performed. The dynamic scan sequence consisted of ten 2-min, ten 4-min and three 10-min scans. The total scan period was 90 min. An additional 15-min static scan was also initiated at 168 min after the start of the infusion.

The ring-type SPET scanner used was the Headtome-II (Shimadzu Corp., Kyoto, Japan [12, 13]), which has three detector rings with 64 NaI rectangular detectors. The spatial resolution at the center of the field of view (FOV) is 8 mm full-width at half-maximum (FWHM), and the slice thickness was 17 mm. Image slices were taken at 7 mm, 42 mm and 77 mm above and parallel to the orbital-meatal (OM) line. The images were reconstructed using filtered backprojection with a Butterworth filter. Attenuation correction was made numerically by assuming an elliptical brain outline.

Frequent arterial blood sampling was performed in this group according to the protocol described for generating the standard input function in Appendix 1. Both the whole blood radioactivity concentration and the octanol extraction fraction were measured for each sample. Two kinds of input functions were obtained: (1) the true input function calculated by multiplying the whole blood radioactivity concentration curve by the octanol extraction fraction in each sample, and (2) the standard input function scaled by a factor determined by the blood sample taken at 10 min after the start of infusion.

Additional blood samples were taken at 5 min, 10 min, 20 min and 60 min after the start of infusion to measure the partial pressure of CO_2 in the arterial blood ($PaCO_2$).

Group 2 (SPET scans using a rotating gamma camera). Two SPET scans were performed in the second group using a Siemens ZLC-7500 rotating gamma camera (spatial resolution: 12 mm FWHM at the centre of FOV; slice thickness: 20 mm). Tomographic images were reconstructed using the same algorithm as described for the first group (repositioned for the delayed scan). The subject was positioned under the gamma camera with the OM line parallel to the detector. SPET scans were acquired starting at 27 min and 167 min following the infusion for approximately 25 min, giving mid-scan times of approximately 40 min and 180 min, respectively. The scans were performed with 18 s data acquisition for each of 64 views, and there was a dead time during the gantry movement. A blood sample (1.5 ml) was taken from the radial artery at 10 min following the injection of IMP, and the standard input function was scaled by measuring its whole blood radioactivity concentration. $PaCO_2$ was also measured using this sample.

Cross-calibration scans in SPET. In order to calibrate the sensitivity between the SPET scanners and the well counter system, a cylindrical uniform phantom (16 cm inner diameter and 15 cm in length) was prepared. Approximately 40 MBq of IMP was stirred in the phantom and a SPET scan was initiated (for 10 min using the Headtome-II and for approximately 25 min using the ZLC-7500). A sample was taken from the phantom after the SPET scan, and its radioactivity concentration was measured using a well counter.

The cross-calibration scans were performed twice before and after collection of all human data (with an interval of approximately 3 weeks). The calibration factor was consistent to within 3% for the two SPET scanners used.

Positron emission tomography. In order to validate the present method, all subjects were studied by PET prior to the SPET study (within 1 h before IMP administration). After a transmission scan for attenuation correction, a 90-s static scan was initiated following a bolus injection of oxygen-15 labelled water ($H_2{}^{15}O$) to calculate the rCBF. The PET scanner used was the Headtome-IV [14] (seven-slice machine), which provided 14 tomographic images at 6.5-mm intervals by the continuous axial motion of the gantry. The image slices were parallel to the OM line (same as for the SPET studies). The rCBF images were calculated according to the autoradiographic method [15–20]. The distribution volume of water was assumed to be 0.80 ml/ml to empirically correct for the tissue heterogeneity in the brain (use of V_d=0.80 ml/ml corrects for systematic underestimation in the calculated rCBF due to the tissue heterogeneity and provides rCBF values which are independent of the scan period [21]). The arterial input function was monitored continuously using a beta probe, and its delay and dispersion were corrected carefully according to our previous works [17–19].

Data analysis. All reconstructed image data (both SPET and PET) were transferred to a UNIX work station (TITAN-750), and all further analyses were done on this system. SPET images were corrected for the radioactive decay of iodine-123 back to the IMP injection start time, normalized by the data collection time, and cross-calibrated to the well counter system. In addition, images obtained from the first group by the dynamic SPET scans were accumulated to provide four static images of 8 min duration and mid-scan times of 10, 20, 60 and 80 min. These accumulated images and the static image taken at 180 min were used for the early and the delayed scan data in the table look-up analysis, respectively.

Regions of interest. Selection of regions of interest (ROIs) was carried out on SPET images by an experienced radiologist in 12 regions of the cortical grey matter, including the cerebellum and territories of the anterior carotid artery, the anterior trunk of the middle carotid artery (MCA), the middle trunk of the MCA, the posterior trunk of the MCA and the posterior carotid artery. Circular ROIs 32 mm in diameter were used for the cerebellar region, and elliptical ROIs for other regions (16 mm in the short axis and 32–34 mm in the long axis). The ROI selection was made independently for both early and delayed SPET scan images. For the data from the first subject group, ROIs were projected onto the dynamic SPET images to provide the time-activity curves for each ROI.

ROIs were also selected on PET-CBF images using the same criteria as for the SPET analysis.

rCBF calculation for dynamic SPET data. The table look-up method was applied to data obtained by dynamic SPET for the following scan combinations: 10 min – 60 min, 20 min – 80 min, 40 min –180 min and 10 min – 180 min, corresponding to the early and

delayed scans, respectively. The calculation was done both by using the standard input function with the calibration sample taken at 10 min following the injection of IMP, and by the direct use of arterial sampling (true input function).

rCBF calculation for data obtained by the rotating gamma camera. The table look-up method was also applied to data obtained by the rotating gamma camera. In this analysis, only the standard input function was used. The standard input function was calibrated using the whole blood radioactivity concentration measured at 10 min following the infusion of IMP.

Non-linear least squares fitting analysis. Non-linear least squares fitting (NLLSF) analyses were performed for time-activity curves generated from the dynamic SPET studies. Two parameters, K_1 and k_2, and three parameters, K_1, k_2 and k_3, were fitted according to the two-compartment model (Eq. 3) and the three-compartment model (Eq. 2), respectively. Then, the relation between the K_1 values calculated by the two-compartment model and those calculated by the three-compartment model was appraised. The magnitude of the k_3 values was also evaluated.

rCBF calculation by the microsphere model. Values of rCBF were also calculated by using the microsphere model for the data obtained from dynamic SPET. Here, the SPET mid-scan time was chosen to be 5 min after the IMP injection (scan duration = 4 min), and rCBF was calculated as follows:

$$f = \frac{C_t(t = 5\,\text{min})}{\int_0^{t=5\,\text{min}} C_a(\tau)d\tau}. \quad (13)$$

Results

Simulation

Figure 2 shows the simulated tissue time-activity curves following the administration of IMP for various rCBF values (V_d was fixed at 30.0 ml/ml). It can be seen that change in the tissue radioactivity concentration is large before 20 min, particularly at a high rCBF range. Because of the requirement of constant radioactive distribution for artefact-free image reconstruction, a short SPET study at a time greater than 20 min is advisable on the basis of these data.

Figure 3 shows typical relations between the early-to-delayed count ratio and the k_2 (f/V_d) value for four scan time combinations. The relation was most linear and steepest for the scan combination of 10–180 min. Scan combinations of 10–60 and 20–80 min also provided linear relations, but they had smaller slopes than the combination of 10–180 min. The scan combination of 40–180 min yielded a relation which was saturated at a high k_2 range. All scan combinations showed monotonic relations for a range of $k_2 < 0.03$ min^{-1}.

Comparison of rCBF values (IMP SPET vs $H_2{}^{15}O$ PET)

Figures 4a and 4b show comparisons of rCBF values calculated by the present method (table look-up method)

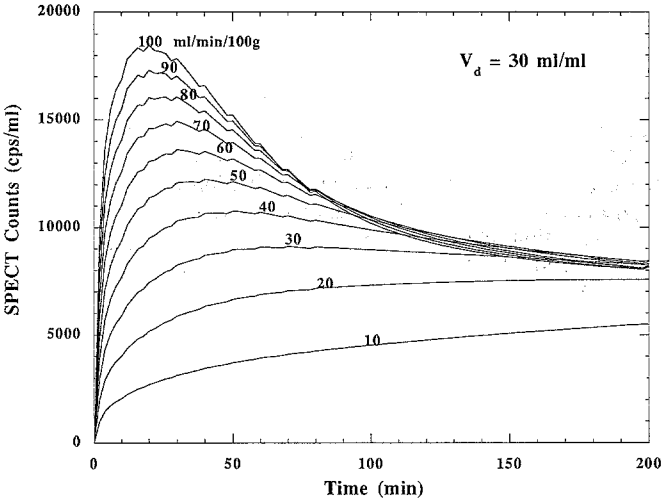

Fig. 2. Simulated tissue time-activity curves following IMP infusion for various rCBF values. The calculation was done for rCBF values from 10 to 100 ml/min per 100 g in steps of 10. The standard input function (a product of the standard whole blood radioactivity concentration and the standard octanol extraction fraction shown in Fig. A1) was used. The V_d value was fixed at 30.0 ml/ml. Because constant radioactivity distribution during the scan is required for accurate image reconstruction, delayed initiation of the SPET scan for a short period is recommended

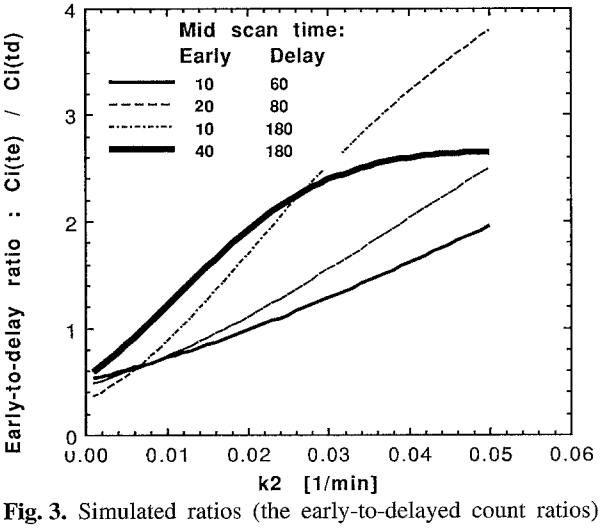

Fig. 3. Simulated ratios (the early-to-delayed count ratios) as a function of k_2 for various scan time combinations (mid-scan times of 10 and 60 min, 20 and 80 min, 10 and 180 min, and 40 and 180 min)

with those calculated by the $H_2{}^{15}O$-PET method. Data shown in Fig. 4a were obtained by use of the Headtome-II (group A), and those shown in Fig. 4b were obtained by the ZLC-7500 (group B). The scan combination used was 40 min and 180 min (mid-scan times) in both sets of data. Significant correlations are observed in both plots. The rCBF values calculated by the table look-up method were slightly smaller than unity (approximately 20% lower than those obtained by $H_2{}^{15}O$-PET).

In Fig. 5, rCBF values calculated by the NLLSF analysis are compared with those calculated by $H_2{}^{15}O$-PET.

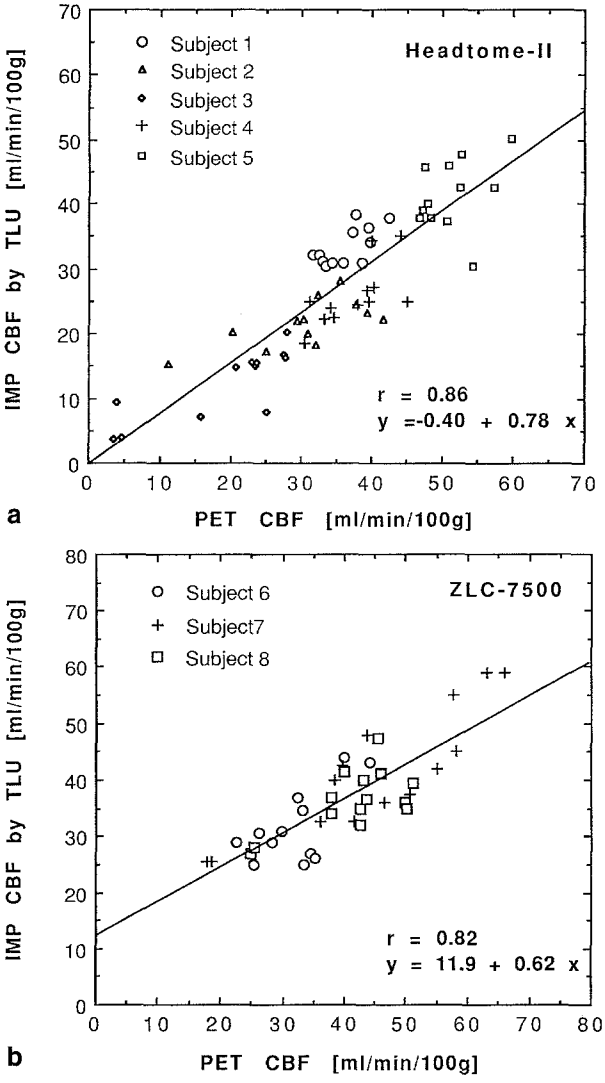

Fig. 4a, b. Comparison of rCBF values obtained by the present method with those obtained by the $H_2{}^{15}O$ PET technique. The IMP rCBF values shown in **a** were obtained from the first group with the Headtome-II scanner (number of ROIs = 60), and those in **b** were obtained from the second group with the rotating gamma camera (n =39). In both figures, the IMP rCBF values were calculated by means of the standard input function with one point calibration using the blood taken at 10 min following infusion of IMP. The SPET scan combination (mid-scan times) was 40 min and 180 min for both figures

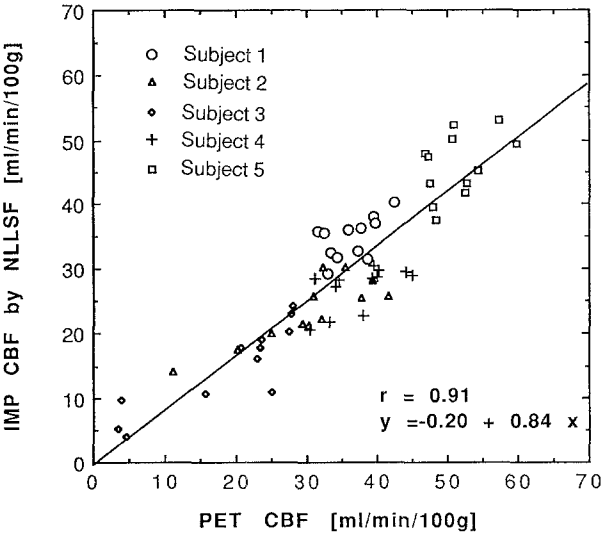

Fig. 5. Comparison of rCBF values calculated by NLLSF analysis for the dynamic SPET data with those calculated by the $H_2{}^{15}O$ PET method. Sixty ROIs were obtained from five subjects. The two-compartment model illustrated in Fig. 1a was used. The true input functions were used in the IMP SPET analysis by measuring the whole blood radioactivity curve and the octanol extraction fraction curve in each study. Note that the correlation coefficient was similar to that shown in Fig. 4a (one blood sampling and two SPET scans with the scan combination of 40–180 min)

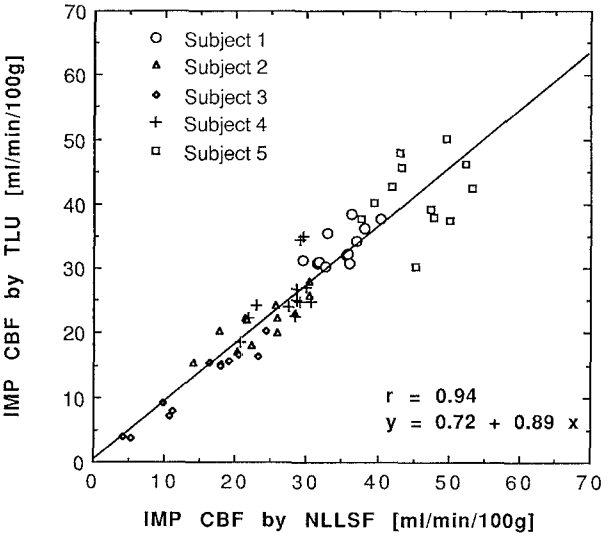

Fig. 6. Comparison of rCBF values obtained by the present method (one blood sampling and 2 SPET scans at 40 and 180 min) with those obtained from the NLLSF analysis. In the NLLSF analysis, the two-compartment model illustrated in Fig. 1a was fitted to the brain time-activity curve and the arterial input function was obtained by frequent arterial blood sampling and measurement of the octanol extraction fraction for each sample

It should be noted that the correlation coefficient (r = 0.91) was similar to that obtained by the table look-up method with the scan combination of 40 and 180 min (r = 0.86) and one blood sampling (Fig. 4a).

Figure 6 shows a comparison of rCBF values obtained by the present method (table look-up method) with those obtained by NLLSF analysis. Agreement between the two analyses suggests consistency of the table look-up method with the NLLSF analysis, thus indicating the validity of avoiding frequent arterial blood sampling and dynamic SPET data acquisition. A comparison of rCBF values obtained by the present method with those obtained by the microsphere model analysis is shown in Fig. 7, again suggesting consistency between the two methods.

Table 2 summarizes correlation coefficients (r values by linear regression analysis) between rCBF values calculated by the table look-up method (for two SPET scan

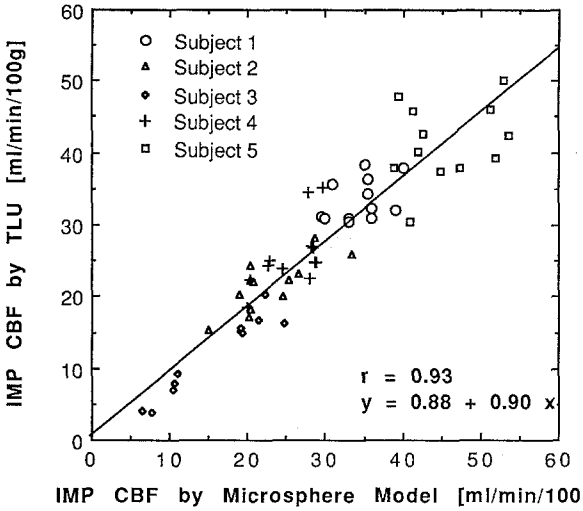

Fig. 7. Comparison of rCBF values obtained by the present method (one blood sampling and 2 SPET scans at 40 and 180 min) with those obtained from the microsphere model analysis, demonstrating consistency between the two methods. In the microsphere model analysis, the SPET mid-scan time was 5 min after the IMP injection (scan duration = 4 min)

Table 2. Summary of linear regression analysis: IMP table look-up method versus $H_2{}^{15}O$-PET method. rCBF values were compared for 60 ROIs obtained from five subjects

Mid-scan times (min)		Correlation coefficient	
Early scan	Delayed scan	Individual input function[a]	Standard input function[b]
10	60	$r = 0.86$	$r = 0.40$[c]
20	80	$r = 0.87$	$r = 0.59$[d]
40	180	$r = 0.84$	$r = 0.86$
10	180	$r = 0.87$	$r = 0.66$[e]

[a] Input function was obtained by frequent arterial blood sampling and measurement of octanol extraction fraction for each sample

[b] Input function was calculated by use of a standard input function. Data of one blood sample were used to normalize the standard input function

[c] The table look-up method failed to calculate rCBF for 11 ROIs, because the early-to-delayed count ratio was out of range for these regions

[d] Values could not be calculated for seven ROIs, for the same reason as given in footnote c.

[e] Values could not be calculated for one ROI for the same reason as given in footnote c.

data) and those calculated by the $H_2{}^{15}O$-PET method. The r values were estimated for four different scan time combinations, i.e. mid-scan times of 10 min and 60 min, 20 min and 80 min, 40 min and 180 min, and 10 min and 180 min, corresponding to the early and delayed scans, respectively. All data were obtained from studies with the Headtome-II (group A). Using the individual arterial input function, relatively good correlations were obtained between IMP-CBF and PET-CBF, and the correlation coefficients were similar for the different scan combinations, ranging from 0.84 to 0.87. On the other hand, when the standard input function was used with one point calibration, the correlation coefficient was sensitive to the scan time combination, and the best correlation was obtained for the scan combination of 40 min and 180 min. The correlation coefficient for this scan combination was similar to that for the individual arterial input function.

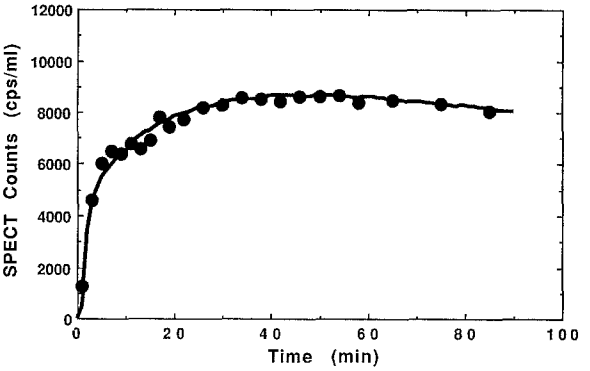

Fig. 8. Typical fit of the regional brain time-activity curve by the two-compartment model. Good agreement suggests the validity of the two-compartment model for describing the kinetics of IMP in the brain

Distribution volume

The V_d value was 30.0 ± 8.3 in the normal region, which showed normal density on X-ray computed tomography (CT) (55 ROIs), and 14.1 ± 3.7 in the infarcted region, which showed low density on X-ray CT (10 ROIs). Student's t test indicated a significant difference between the two regions ($P<0.001$).

Two-compartment model versus three-compartment model

Figure 8 shows a typical fit by the NLLSF analysis based on the two-compartment model illustrated in Fig. 1a. Results of the NLLSF analysis based on the two-compartment model (Fig. 1a) are compared with those based on the three-compartment model (Fig. 1b) in Fig. 9. The calculated K_1 values correlated and agreed well with each other (r = 0.92). The two-compartment model analysis produced only a slightly larger K_1 value than the three-compartment model analysis (by a factor of approximately 8%). Values of k_3 calculated with the three-compartment model analysis were (mean ±1 SD) 0.0056 ± 0.0128 (36 ROIs), and were not significantly different from zero.

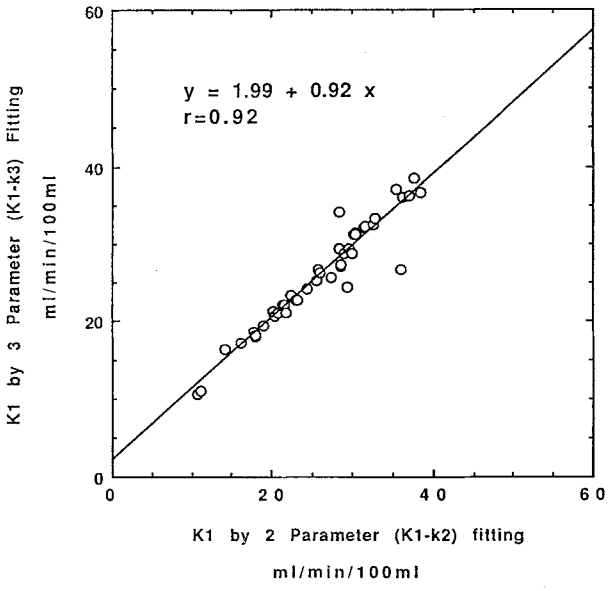

Fig. 9. Comparison of K_1 values obtained by the NLLSF analysis (n = 60 ROIs from five subjects). Values denoted on the x-axis were obtained based on the two-compartment model with two parameters (K_1 and k_2), and values on the y-axis were obtained based on the three-compartment model with three parameters (K_1, k_2 and a retaining rate constant k_3). Both K_1 values were in good agreement with each other (only 8% difference), suggesting that inclusion of k_3 increases only a noise fraction but does not improve the systematic error which may be caused by neglecting the retaining rate constant. The arterial input function was obtained from frequent arterial blood sampling and the octanol extraction fraction was measured for each sample. This figure shows the empirical validation of the two-compartment model for describing the IMP kinetics in the brain

Discussion

Table look-up method

This article describes a new method for measuring the rCBF quantitatively using IMP and a rotating gamma camera for a given ROI. The clearance of IMP from the brain, which can cause a systematic underestimation of the calculated rCBF value and reduction of the contrast between high and low rCBF areas [6, 8], has been corrected by employing the two-compartment model shown in Fig. 1a. Two values of rCBF and the regional distribution volume of IMP were calculated by implementing the table look-up procedure for each ROI. It has been confirmed that the rCBF values obtained by the present method are consistent with those obtained by the $H_2{}^{15}O$-PET technique, suggesting that this method is accurate.

To minimize the technical procedures, the number of required SPET scans was reduced to two, which was the minimum number for solving two unknown parameters in the model equation (note that calculation of two parameters from one tracer administration normally requires dynamic data acquisition). The suggested scanning time points of 40 and 180 min following the administration of IMP (see below) can be achieved using a conventional rotating gamma camera. The generation and use of a standard input function prior to the study and calibration of it by one point blood sampling were validated. This avoids the need for frequent arterial blood sampling and measurement of the lipophilic component for each sample. Two polynomial functions were developed for the table look-up procedure, which avoided the need for development of a sophisticated program. These simplified procedures are of great advantage for clinical application.

One of the reasons for underestimation (by a factor of approximately 20%) of rCBF values obtained by this technique compared with those obtained by the $H_2{}^{15}O$-PET technique was probably the limited first-pass extraction fraction (E) of IMP. In this article, E was assumed to be unity when calculating the rCBF value from K_1 (Eq. 2a). However, it has been reported by Kuhl et al. [2] that E is 0.92 and 0.74 for hemispheric rCBF of 0.33 and 0.66 ml/min per g, respectively. Other investigators [22] have also reported the permeability-surface area (PS) product for IMP to be 93.4 ml/100 g per min; hence the Renkin-Crone equation ($E=1-e^{-\frac{PS}{f}}$) yields a first-pass extraction fraction of approximately 0.85 at f=50 ml/min per 100 g [23, 24]. Another reason for the systematic underestimation of rCBF may be the poorer spatial resolution of the SPET scanner compared with the PET scanner. The limited spatial resolution causes a systematic underestimation of the radioactivity concentration in the grey matter region and cross-contamination between the grey and the white matter. Both factors (underestimation of radioactivity concentration and tissue mixture) are expected to cause systematic underestimation of the calculated rCBF values [9, 25]. The exact magnitude of the underestimation is, however, unknown, and most likely patient and ROI dependent. A further study should be performed to evaluate the effects of the lower spatial resolution of SPET as compared with PET.

Optimal SPET scan times

The present method requires the performance of two SPET scans after the administration of IMP. The scan times are in theory arbitrary for providing both rCBF and V_d values. However, it has been demonstrated in Table 2 that the agreement between rCBF values obtained with the present method and with the $H_2{}^{15}O$-PET technique was dependent on the scan time combination, with the combination of 40–180 min yielding the best correlation with the reference method. The following factors are related to the optimal SPET scan times:

1. Error sensitivity to the statistical noise
2. Error sensitivity to the individual difference in the input function
3. Error sensitivity to change of radioactivity distribution during the SPET scan

The most linear and steepest relationship of early-to-delayed count ratio and k_2 (Fig. 3) is preferred in order to minimize the error sensitivity to the statistical noise in the observed count ratio in the table look-up procedure. From this point of view, it is recommended that the first scan be performed at the extremely early phase and that the second scan be performed at the latest period, e.g. a scan combination of 10 min and 180 min. However, this combination increases the errors due to the second and third factors listed above. The convolution integral for the early scan time, $\Gamma = \rho \cdot C_a(t_e) \otimes e^{-\frac{f}{V_d} \cdot t_e}$, is sensitive to individual differences in the input function when the scan is performed at the extremely early phase. From this point of view, the first scan is best performed as late as possible in order to minimize the inter-individual difference in the integration of the input function. Another disadvantage of early commencement of the first scan derives from the change in the radioactivity distribution in the brain, particularly at a high rCBF range (see Fig. 2). Quantitative image reconstruction requires a constant radioactivity distribution during the scan. The tracer concentration in the brain is relatively constant at 40 min after IMP administration, allowing the use of a conventional rotating gamma camera. It is probable that these factors caused the scan combination of 40 min and 180 min to provide the best correlation with the PET technique.

Optimal blood sampling time

In this article, the time of the blood sample for calibrating the standard input function was determined so as to minimize the difference of integration of the calculated input function from that of the true input function. It should be noted that, in the conventional microsphere model developed by Kuhl et al. [2], calculated CBF value is proportional to the inverse of the integration of the input function. Hence, this process was roughly equivalent to the optimization of the blood sampling time for minimizing the error in the calculated rCBF value due to the individual difference in the input function.

Validity of the two-compartment model

Although there is not a clear physiological justification for use of the two-compartment model for description of the IMP kinetics in the brain, empirical validity has been demonstrated in this article, i.e. (1) the observed tissue time-activity curve is well explained by the two-compartment model equation (Fig. 8), (2) no significant difference was observed between the K_1 values calculated with the two analyses based on the two- and three-compartment models, and (3) the k_3 value was not significantly different from zero. It should be noted that this justification included the data for the pathological and normal regions. These observations suggested that inclusion of k_3 (retention rate constant of IMP in the brain) increases only the statistical uncertainty, and does not improve the systematic error which might be caused by ignoring the retention of IMP.

The validity of the two-compartment model has also been suggested previously by Yokoi et al. [9], They have implemented a unique approach to analyse dynamic IMP data based on a graphical plot, and proved empirically that IMP follows the two-compartment model kinetics even 180 min after the administration of IMP. A systematic error can be caused by the tissue heterogeneity, but the magnitude of the error was found to be small (less than 5%) in the calculated rCBF value.

Sources of error

The following sources of error can be expected in the present method and should be discussed:

1. Limited first-pass extraction of IMP in the brain
2. Limited reproducibility of selecting ROIs in the same location on two SPET images
3. Difference in individual input function from the standard
4. Saturated table at high rCBF range
5. Change in rCBF during the study
6. Limited spatial resolution of SPET
7. Limited physical accuracy in the SPET reconstruction

The first-pass extraction fraction of IMP could be corrected by assuming the PS product; however, this assumed value may not apply to the diseased regions. In order to minimize the error due to the second factor, selection of a reasonably large ROI may be recommended. As for the third factor, further studies would be required because of the limited number of subjects in this article. However, it should be noted that reasonable agreement was observed compared with the reference method ($H_2{}^{15}O$-PET) even for a patient who had severe heart failure (HYHA grade 3, subject 3 in Table 1). In this patient, the input function measured by the frequent arterial sampling showed a significant delay (by approximately 2 min) and dispersion (ca. 50% increase in FWHM). The good agreement in the calculated rCBF value was due to the low sensitivity of the convolution integral to the distortion of the individual input function when the scan was made at 40 min and 180 min. The saturated relationship of k_2 and the early-to-delayed count ratio (fourth factor) can cause an increase in fluctuation at a high rCBF range, but this might be less of a problem when calculating rCBF values for diseased regions. Change in rCBF may be caused between the two SPET scans, particularly if the patient is repositioned. However, the effects of such a change in rCBF are probably not significant, because the brain tissue (particularly cortical grey matter) is unlikely to accumulate or lose large

amounts of radioactivity during the wash-out phase after the early scan period even with a large change in rCBF. This is because, firstly, the amount of IMP transported from the blood to the brain is small due to the low blood radioactivity concentration, and secondly, clearance of the tracer is in general less sensitive to the change in rCBF for V_d of approximately 30 ml/ml. Limited spatial resolution of the SPET scanner causes non-negligible effects of tissue mixture (e.g. mixture of grey and white matter). This can cause systematic error (underestimation) in the estimation of the average rCBF over the selected ROI. Further study is required to investigate this effect. The last factor listed above includes incomplete corrections for the attenuation of gamma rays and the scatter, in particular, in the deep grey matter regions such as the basal ganglia. It would be highly desirable to improve the physical accuracy in the SPET reconstruction.

The future

In this study the blood sample for calibration of the standard input function was taken from the radial artery at 10 min following the administration of IMP. This arterial blood sampling can be replaced by venous blood sampling, which would be of great advantage in the clinical setting. Arterialized venous blood sampling is frequently performed in PET studies for fluorodeoxyglucose and other tracers. In fact, we confirmed in one study that the venous radioactivity concentration measured at t=10 min was in good agreement with the arterial blood radioactivity concentration taken at the same time (difference <2%). The optimal time for venous blood sampling to minimize the calibration error might, however, be slightly later than that estimated for arterial sampling (10 min post administration) because of distortion of the blood time-activity curve around the peak. Further studies should be performed to confirm this.

It has been demonstrated that the V_d values are significantly different between normal and infarcted regions. Although the physiological meaning of V_d is not yet clear, it is expected that the region showing preserved V_d values, even though rCBF is reduced, has normal tissue density (fraction of non-scar tissue), and that this may indicate the viable tissue surrounding the infarcted region. It would be important to evaluate further the clinical significance of the V_d value in the border zone, such as the ischaemic penumbra zone.

Conclusion

A method has been developed to measure rCBF and V_d from one blood sampling and two SPET scans for a given ROI. Clearance of IMP from the brain was taken into account by employing the two-compartment model. The present study demonstrated that the obtained rCBF values agree well with those measured by the $H_2{}^{15}O$ PET method, suggesting the validity of this method. There was no significant difference between the rCBF values calculated using the two-compartment model and those calculated using the three- compartment model, suggesting the empirical validity of use of the two-compartment model to describe the IMP kinetics. Use of the standard input function avoided frequent arterial blood sampling and separation of the lipophilic fraction. It was suggested that the blood sampling should be performed at 10 min following IMP infusion, and the two SPET scans at 40 and 180 min, respectively. Relatively delayed timing of the SPET scans allows use of a conventional rotating gamma camera for quantitative measurement of rCBF. It was also found that V_d values measured by the present method were significantly reduced in infarcted regions compared with normal regions, indicating the importance of simultaneous determination of rCBF and V_d values for each region.

Acknowledgements. We wish to thank the staff of the Research Institute for Brain and Blood Vessels, Akita, in particular Messrs. Takenori Hachiya and Yasuaki Shoji for handling the SPET and PET scanners. This work was supported in part by a grant from the Japan Heart Foundation, Grant for 1990, and in part by Targeted Institutional Links Program – Department of Employment Education and Training, Australian Government. This work was previously presented at the 39th Annual Meeting of the Society of Nuclear Medicine, held in Los Angeles in 1992 [26].

Appendix 1
Generation of the standard input function

A standard input function of IMP has been generated prior to the study. The subjects consisted of eight male normal volunteers and four patients with chronic cerebral infarction. Their ages ranged from 31 to 72 years (average: 55). None of the subjects showed any abnormality in their lung or cardiac function. Five were smokers. 222 MBq of IMP (111 MBq in four cases, the input data being scaled so as to be equivalent to 222 MBq) was infused into the antecubital vein continuously at a constant infusion rate using a Harvard pump for a period of 1.0 min. Following the start of infusion, arterial blood (approximately 1.5 ml) was sampled frequently from the radial artery. The sampling period was within 2 s for all samples. The sampling time was every 15 s for the first 2 min; the interval was then gradually prolonged, until 90 min. One more sample was taken at 180 min from the antecubital vein (on the other side from the IMP infusion). For all blood samples, the whole blood radioactivity concentration (cps/g) was counted, and their octanol extraction fraction (lipophilic fraction) measured [2].

Figure A1 shows the arterial whole blood radioactivity concentration curve and the octanol extraction fraction curve, averaged for all 12 subjects. The averaged whole blood radioactivity concentration at 180 min was 256 cps/ml, and the octanol extraction fraction 0.49. The

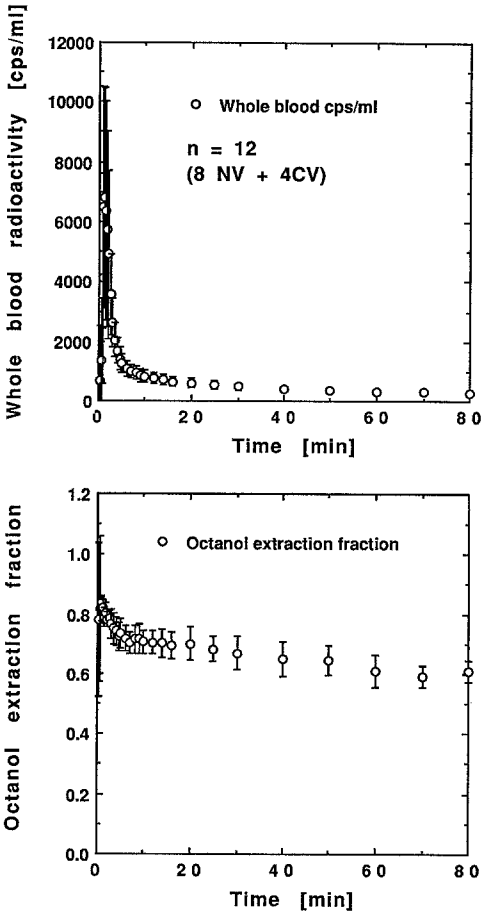

Fig. A1. Standard whole blood radioactivity curve (*above*) and octanol extraction fraction (below) obtained from 12 human studies (eight normal volunteers and four cerebrovascular patients) following IMP administration. The product of these two curves provides a standard shape of the input function. One blood sampling was performed in each study, and whole blood radioactivity was measured to calibrate this standard input function. *Bars* correspond to the standard deviation at each time. The whole blood radioactivity and the octanol extraction fraction at t=180 min were 250 ± 39 cps/ml and 0.50 ± 0.039, respectively

product of these two curves corresponds to the true input function for IMP.

Appendix 2
Determination of the calibration time for the standard input function

The blood sampling time for calibration of the standard input function was determined by optimizing the following cost function:

$$\Omega(t) \equiv \frac{1}{12}\sum_{i=1}^{12}\frac{\left|\int_0^T C_a(s)ds - \int_0^T X^i(t)\cdot A(s)ds\right|}{\int_0^T C_a(s)ds}, \qquad \text{(A1)}$$

where $X^i(t)$ denotes the calibration factor calculated as the ratio of counts at time t (ratio of the whole blood

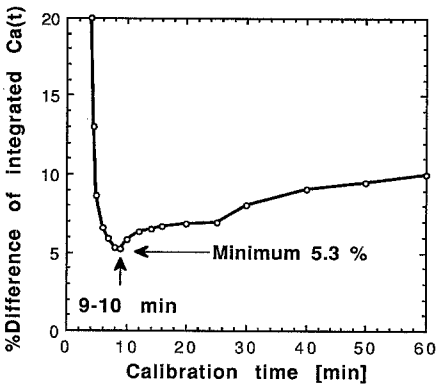

Fig. A2. Optimization of the blood sampling time for calibration of the standard input function. The cost function that has been minimized was the inter-individual difference in the integration of the input function. The minimum value of 5.3% was obtained when the calibration was done at between 9 and 10 min after the IMP infusion. The cost function is formulated in Eq. A1

counts in each subject to that in the standard whole blood curve) and T is the integration period for both input functions (each individual function and the calibrated standard function). In this study, the integration time, T, was set at 40 min. This cost function is the difference of integration (from zero to 40 min) of the standard input function calibrated by the counts at time t from that of the true input function measured directly by the frequent arterial sampling. The minimization of this cost function as a function of the calibration time, therefore, corresponds to the optimal calibration time, which yields the minimum error in the integration of the arterial input function.

Figure A2 shows a plot of the cost function, Ω (t), as a function of the calibration time. It can be seen that the minimum value (approximately 5.3%) was obtained when the calibration time was between 9 and 10 min after the infusion of IMP. The error increased gradually when the calibration time was later than 10 min, and increased immediately when the calibration time was before 9 min.

Appendix 3
Table look-up calculation using polynomial functions

The present method requires generation of two tables prior to the ROI analysis, namely a relation between the early-to-delayed count ratio (on the right side of Eq. 5 and the f/V_d value, and a relation between the convolution integral ($\rho \cdot C_a(t_e) \otimes e^{-\frac{f}{V_d}\cdot t_e}$, defined as Γ in Eq. 7) at the early mid-scan time and the f/V_d value. For a given input function and a given scan time combination, these two tables become unique, and only dependent on a constant factor for calibrating the individual input function. Because of this, generation of the tables is required only once, and the table look-up procedure can be replaced by

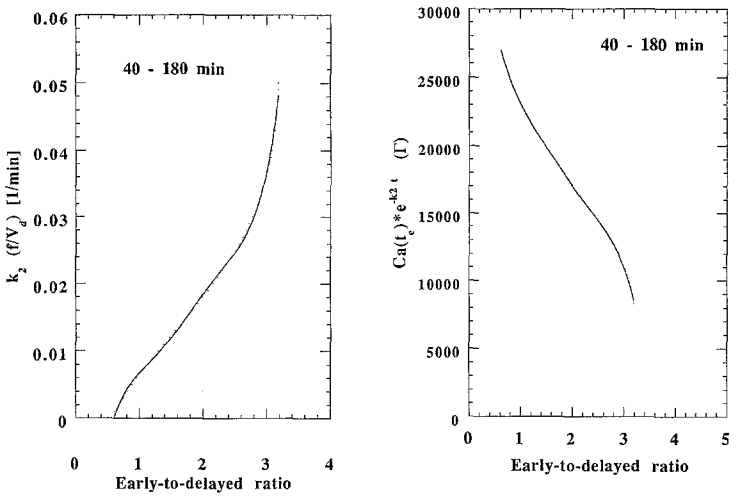

Fig. A3. Simplification of the table look-up procedure by use of two polynomial equations. Values of k_2 (f/V_d) and Γ (the convolution integral) are replaced by two polynomial equations as described in Appendix 3, and can be calculated from the early-to-delayed count ratio. The accuracy of these polynomial functions (five order) was less than 2% for a reasonable range

Table A1. Constant factors in polynomial equations (A2 and A3) which describe values of f/V_d and Γ for scan combinations

Early MST (min)	Delayed MST(min)	m_0	m_1	m_2	m_3	m_4	m_5
10	60	− 0.040494	+ 0.11819	− 0.099881	+ 0.06065	− 0.019667	− 2.6718 10^{-3}
20	80	− 0.033093	− 0.080931	− 0.057561	+ 0.03027	− 0.008497	+ 1.0454 10^{-3}
40	180	− 0.047253	+ 0.15931	− 0.195045	+ 0.121179	− 0.036247	+ 4.1532 10^{-3}
110	180	− 0.007483	+ 0.02823	− 0.014048	+ 0.00506	− 8.749 10^{-4}	+ 6.1309 10^{-5}

Early MST (min)	Delayed MST (min)	n_0	n_1	n_2	n_3	n_4	n_5
10	60	+ 20781.4	− 14445.68	+ 13625.0	− 8379.47	+ 2751.219	− 372.8011
20	80	+ 32014.3	− 28185.14	+ 22815.9	− 1593.811	+ 3119.451	− 348.0232
40	180	+ 43301.1	− 45911.75	+ 44139.0	− 24485.46	+ 6795.586	− 745.6684
10	180	+ 16879.5	− 3030.615	+ 1584.69	− 67.1824	+ 98.95825	− 6.854497

MST, Mid-scan time

a simple numerical calculation by preparing polynomial functions prior to the study as follows:

f/V_d and Γ for a scan combination of 40–180 min were plotted in Fig. A3 as a function of the early-to-delayed counts ratio, where the standard input function described in Appendix 1 was used. In this Appendix, these tables for each scan combination were fitted by five-order polynomial functions:

$$f/V_d = m_0 + m_1 X + m_2 X^2 + m_3 X^3 + m_4 X^4 + m_5 X^5 \quad \text{(A2)}$$

and

$$\Gamma = n_0 + n_1 X + n_2 X^3 + n_3 X^3 + n_4 X^4 + n_5 X^5, \quad \text{(A3)}$$

where X denotes the early-to-delayed count ratio for a given scan time combination, and m_0 to m_5 and n_0 to n_5 are constant factors which are only dependent on the scan time combination. Values of m_0 to m_5 and n_0 to n_5 are summarized in Table A1 for scan combinations of 10–60 min, 20–80 min, 40–180 min and 10–180 min.

References

1. Winchell HS, Horst WD, Braun L, Oldendorf WH, Hattner R, Parker H. *N*-Isopropyl [^{123}I]*p*-iodoamphetamine: single-pass brain uptake and washout; binding to brain synaptosomes; and localization in dog and monkey brain. *J Nucl Med* 1982; 21: 947–952.
2. Kuhl DE, Barrio JR, Huang SC, Selin C, Ackermann RF, Lear JL, Wu JL, Lin TH, ME Phelps. Quantifying local cerebral blood flow by *N*-isopropyl-*p*(I-123) iodoamphetamine tomography. *J Nucl Med* 1982; 23: 196–203.
3. Podreka I, Baumgartner C, Suess E, Muller C, Brucke T, Lang W, Holzner F, Steier M, Deecke L. Quantification of regional cerebral blood flow with IMP-SPECT: reproducibility and clinical relevance of flow values. *Stroke* 1989; 20: 183–191.
4. Creutzig H, Schober O, Gielow P, Friedrich R, Becker H, Dietz H. Cerebral dynamics of *N*-isopropyl-(^{123}I)*p*-iodoamphetamine. *J Nucl Med* 1986; 27: 178–183.
5. Nishizawa S, Tanada S, Yonekura Y, Fujita T, Mukai T, Saji H. Regional dynamics of *N*-isopropyl-(^{123}I)*p*-iodoamphetamine in human brain. *J Nucl Med* 1989; 30: 150–156.
6. Greenberg JH, Kushner M, Rango M, Alavi A, Reivich M. Validation studies of iodine-123-iodoamphetamine as a cere-

bral blood flow tracer using emission tomography. *J Nucl Med* 1990; 31: 1364–1369.
7. Matsuda H, Higashi S, Tsuji S. A new noninvasive quantitative assessment of cerebral blood flow using *N*-isopropyl-(iodine 123)*p*-iodoamphetamine. *Am J Physiol Imaging* 1987; 2: 49–55.
8. Murase K, Tanada S, Mogami, Kawamura M, Miyagawa M, Yamada M, Higashino H, Iio A, Hamamoto K. Validity of microsphere model in cerebral blood flow measurement using *N*-isopropyl-*p*-(I-123) iodoamphetamine. *Med Phys* 1990; 17: 79–83.
9. Yokoi T, Iida H, Itoh , H, Kanno I. A new strategy based on graphical plot analysis for rCBF and partition coefficient with iodine-123 IMP and dynamic SPECT: validation study using O-15 water and PET. *J Nucl Med* 1993; 34: 498–505.
10. Takeshita G, Maeda H, Nakane K, Toyama H, Sakakibara E, Komai S, Takeuchi A, Koga S, Ono M, Nakagawa T. Quantitative measurement of regional cerebral blood flow using *N*-isopropyl-(iodine-123)*p*-iodoamphetamine and single-photon emission computed tomography. *J Nucl Med* 1992; 33: 1741–1749.
11. Itoh H, Iida H, Bloomfield PM, Murakami M, Higano S, Kanno I, Fukuda H, Uemura K. A technique for a rapid imaging of rCBF and partition coefficient using dynamic SPECT and I-123-amphetamine (IMP). *J Nucl Med* 1992; 33 (Suppl): 911.
12. Kanno I, Uemura K, Miura S, Miura Y. Headtome: A hybrid emission tomography for single photon and positron emission imaging of the brain. *J Comput Assist Tomogr* 1981; 5: 216–226.
13. Hirose Y, Ikeda Y, Higashi Y, Koga K, Hattori H, Kanno I, Miura Y, Miura S, Uemura K. A hybrid emission CT-Headtome II. *IEEE Trans Nucl Sci* 1982; NS-29: 520–523.
14. Iida H, Miura S, Kanno I, Murakami M, Takahashi K, Uemura K, Hirose Y, Amano M, Yamamoto S, Tanaka K. Design and evaluation of Headtome-IV, a whole-body positron emission tomograph. *IEEE Trans Nucl Sci* 1989; NS-36: 1006–1110.
15. Herscovitch P, Markham J, Raichle ME. Brain blood flow measured with intravenous $H_2{}^{15}O$. I. Theory and error analysis. *J Nucl Med* 1983; 24: 782–789.
16. Raichle ME, Martin WR, Herscovitch P, Markham J. Brain blood blow measured with intravenous $H_2{}^{15}O$. II. Implementation and validation. *J. Nucl Med* 1983; 24: 790–798.
17. Kanno I, Iida H, Miura S, Murakami M, Takahashi K, Sasaki H, Inugami A, Shishido F, Uemura K. A system for cerebral blood flow measurement using an $H_2{}^{15}O$ autoradiographic method and positron emission tomography. *J Cereb Blood Flow Metab* 1987; 7: 143–153.
18. Iida H. Kanno I. Miura S, Murakami M, Takahashi K, Uemura K. Error analysis of a quantitative cerebral blood flow measurement using $H_2{}^{15}O$ autoradiography and positron emission tomography: with respect to the dispersion of the input function. *J Cereb Blood Flow Metab* 1986; 6: 536–545.
19. Iida H, Higano S, Tomura N, Shishido F, Kanno I, Miura S, Murakami M, Takahashi K, Sasaki H, Uemura K. Evaluation of regional difference of tracer appearance time in cerebral tissues using [^{15}O]water and dynamic positron emission tomography. *J Cereb Blood Flow Metab* 1988; 8: 285–288.
20. Iida H, Kanno I, Miura S, Murakami M, Takahashi K, Uemura K. A determination of regional brain/blood partition coefficient of water using dynamic positron emission tomography. *J Cereb Blood Flow Metab* 1989; 9: 874–885.
21. Iida H, Kanno I, Miura S. Rapid measurement of cerebral blood flow with positron emission tomography. *CIBA Found Symp* 163: 23–42.
22. Murase K, Tanada S, Inoue T, et al. Measurement of the blood-brain barrier permeability of I-123 IMP, Tc-99m HMPAO and Tc-99m ECD in the human brain using compartment model analysis and dynamic SPECT. *J Nucl Med* 1991; 32 (Suppl): 911.
23. Renkin EM. Transport of potassium-42 from blood to tissue in isolated mammalian skeletal muscles. *Am J Physiol* 1959; 197: 1205–1210.
24. Crone C. The permeability of capillaries in various organs as determined by use of the indicator diffusion method. *Acta Physiol Scand* 1963; 58: 292–305.
25. Huang SC, Mahoney DK, Phelps ME. Quantitation in positron emission tomography. 8. Effects of nonlinear parameter estimation on functional images. *J Comput Assist Tomogr* 1987; 1: 314-325.
26. Iida H, Itoh H, Munaka, M, Murakami M, Higano S, Murakami M, Uemura K. A clinical method to quantitate CBF using a rotating gamma camera and I-123-amphetamine (IMP) with one blood sampling. *J Nucl Med* 1992; 33: (Suppl): 963.